

Carbohydrate-Based Nanocarriers Exhibiting Specific Cell Targeting with Minimum Influence from the Protein Corona**

Biao Kang, Patricia Okwieka, Susanne Schöttler, Svenja Winzen, Jens Langhanki, Kristin Mohr, Till Opatz, Volker Mailänder, Katharina Landfester,* and Frederik R. Wurm*

Abstract: Whenever nanoparticles encounter biological fluids like blood, proteins adsorb on their surface and form a so-called protein corona. Although its importance is widely accepted, information on the influence of surface functionalization of nanocarriers on the protein corona is still sparse, especially concerning how the functionalization of PEGylated nanocarriers with targeting agents will affect protein corona formation and how the protein corona may in turn influence the targeting effect. Herein, hydroxyethyl starch nanocarriers (HES-NCs) were prepared, PEGylated, and modified on the outer PEG layer with mannose to target dendritic cells (DCs). Their interaction with human plasma was then studied. Low overall protein adsorption with a distinct protein pattern and high specific affinity for DC binding were observed, thus indicating an efficient combination of “stealth” and targeting behavior.

Nanomedicine is a key technology for the 21st century. Besides the initial development of various nanocarrier systems and the development of specific targeting, the development of protein-repellent surfaces is of high importance. When synthetic nanocarriers enter biological fluids, it is known that, due to high surface energy and hydrophobic interactions, they strongly adsorb plasma proteins.^[1] Many researchers have proposed that the in vivo fate of any nanocarrier is determined by this protein “corona”, formed post injection, instead of the intrinsic properties of the (mostly polymeric) nanocarrier.^[2] PEGylation (PEG = poly-

ethylene glycol) is the state-of-the-art approach to reducing nonspecific interactions with plasma proteins; this effect is often termed the “stealth effect”.^[3] However, the stealth effect alone is not enough: specific targeting agents have to be attached additionally in order to reach the binding target.^[1a] But how does this additional moiety interact with plasma proteins? A new corona could be generated, thereby altering the in vivo performance by covering and deactivating the targeting group.

The formation of a protein corona around single-component nanoparticles (NPs), such as polystyrene,^[2c,g,4] zinc oxide,^[5] silica,^[2g,5,6] gold,^[2o,7] silver,^[2o] and titanium dioxide^[2n,5] nanoparticles, has been extensively studied, while the surface modification of nanoparticles with PEG^[8] and zwitterionic agents^[9] has been proven to effectively reduce the protein absorption. However, the combination of “stealth” behavior with “on top” attachment of specific targeting groups has not been studied. The protein interactions of a PEGylated nanocarrier before and after the attachment of an additional targeting group are of central importance for the generation of efficient specific cellular uptake after blood contact. For the first time, we compare the blood plasma interaction of PEGylated nanocarriers with that of nanocarriers that carry mannose groups attached to the PEG chains. Isothermal titration calorimetry (ITC), dynamic light scattering (DLS), and cellular uptake studies before and after incubation with human plasma were performed and the influence on the targeting of dendritic cells was evaluated. In addition, proteomic mass spectrometry revealed a distinct pattern of plasma proteins still present on all of the nanocarriers that does not hamper the specific lectin binding of mannose.

We have been studying hydroxyethyl starch nanocapsules (HES-NCs) as biodegradable nanocarriers intensively.^[10] They are prepared through an inverse miniemulsion method, can be loaded with hydrophilic cargo, and their diameters can be adjusted precisely. More recently, well-controlled PEGylation of HES-NCs was accomplished through a number of different methods.^[11] Herein, we extend these methods to generate nanocarriers that can be further functionalized at the outer layer with specific targeting groups. PEG diisocyanate (OCN-PEG₁₁₀-NCO, $M_n = 5000 \text{ g mol}^{-1}$) reacts with the surface hydroxy groups of the polysaccharide and subsequently with the targeting groups. After one of the isocyanate groups has reacted with the surface, the reactivity of the other one is drastically decreased owing to steric hindrance and loss of mobility. If an excess of PEG diisocyanate is used, there is a further reduction in the formation of cyclic species and the second isocyanate group

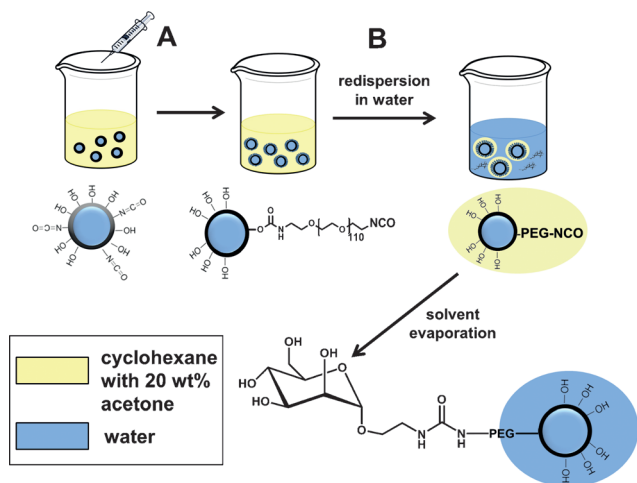
[*] B. Kang, P. Okwieka, S. Schöttler, S. Winzen, Dr. K. Mohr, Dr. V. Mailänder, Prof. Dr. K. Landfester, Dr. F. R. Wurm
Max Planck Institute for Polymer Research
Ackermannweg 10, 55128 Mainz (Germany)
E-mail: landfester@mpip-mainz.mpg.de
wurm@mpip-mainz.mpg.de

P. Okwieka, Dr. V. Mailänder
Department of Hematology, Medical Oncology, and Pneumology
University Medical Center Mainz
Langenbeckstr. 1, 55131 Mainz (Germany)
Dipl.-Chem. J. Langhanki, Prof. Dr. T. Opatz
Institute of Organic Chemistry, University of Mainz
Duesbergweg 10–14, 55128 Mainz (Germany)

[**] Financial support by the BMBF (Cluster CI3) and the DFG (Collaborative Research Project SFB1066) is highly appreciated. We would like to thank Christine Rosenauer for the DLS measurement, and Katja Klein for the synthesis of polystyrene nanoparticles used in this study. F.R.W. thanks the Max Planck Graduate Center for support.

Supporting information for this article is available on the WWW under <http://dx.doi.org/10.1002/anie.201502398>.

remains available for further reactions. Methoxy polyethylene glycol isocyanate ($\text{MeO-PEG}_{110}\text{-NCO}$, $M_n = 5000 \text{ g mol}^{-1}$) was used to prepare PEGylated NCs as control samples for further studies. Quantification of the degree of PEGylation of the NCs was conducted by NMR spectroscopy^[11] and approximately 5×10^5 PEG chains were coupled to the surface for both mono- and difunctional PEGs (Table S1 in the Supporting Information), which is a first indication that PEG diisocyanate reacts selectively at one chain end without the formation of cyclic species. To attach additional targeting groups, different synthetic routes were investigated. Various small biomolecules, such as folic acid,^[10,12] glucose,^[13] mannose,^[14] galactose,^[14a] and disaccharides,^[15] are known to bind selectively to receptors on the cell surface. The coupling of these targeting agents to NCs often involves several reaction steps and quantification is often challenging. Herein, a robust method for the coupling of such small biomolecules to the surface of nanocarriers (Scheme 1) is presented that allows precise quantification of the number of coupled biomolecules.



Scheme 1. General method for the coupling of mannose to HES NCs via isocyanate chemistry. Reactants: A: Diisocyanate-PEG ($\text{OCN-PEG}_{110}\text{-NCO}$, $M_n = 5000 \text{ g mol}^{-1}$) in acetone; B: D-mannosamine or 2-aminoethyl α -D-mannopyranoside in water, followed by evaporation of cyclohexane and dialysis.

Owing to the fast kinetics of the reaction between isocyanates and amines,^[16] amino-functionalized mannose derivatives are directly coupled to the available NCO groups during the redispersion procedure without the need for an additional protective group (Scheme 1). The amino-functionalized carbohydrates will preferably react with the nanocarriers before hydrolysis of the isocyanates occurs. The amount of amine-functionalized mannose in water (before the addition of NCs) can be quantified by the fluorescamine assay (see the Supporting Information).^[17] After the coupling reaction, the NCs are precipitated by centrifugation and the remaining mannose concentration in the solution is quantified by the same method to give the coupling efficiency.

Two different mannose derivatives were used: D-mannosamine and 2-aminoethyl α -D-mannopyranoside, with the amine groups at the C-2 or the C-1 position (the functional-

ized HES-NCs are named HES-PEG5000-C2-Man and HES-PEG5000-C1-Man, accordingly). With this simple and fast method, approximately 2×10^5 mannose units (Table S1 in the Supporting Information) can be attached to each NC. Note that copper-free click chemistry was also studied and led to a 200 times lower mannose density than the isocyanate route (see the Supporting Information). This general method can be used for any type of small biomolecule, as long as it carries an amine group.

The binding affinity of the mannose-functionalized HES-NCs for immature dendritic cells (iDCs) was investigated by fluorescence-activated cell sorting (FACS; Figure S1 in the Supporting Information). In a recent study, our group demonstrated that unmodified HES-NCs show a low degree of unspecific cell uptake.^[10] Besides the low uptake of HES-NCs “as prepared”, subsequent PEGylation of the NCs further reduces the uptake into iDCs (Figure S1). Furthermore, the NCs modified through the click method (HES-PEG5000-DBCO-Man) exhibited a similar low uptake into dendritic cells as the HES-PEG5000. This is attributed to the rather low density of targeting units per capsule (0.0028 mannose units per nm^2). The interaction between the receptor and a single carbohydrate molecule is inherently weak and has a binding constant in the range of 10^3 – 10^4 L mol^{-1} . Upon increasing the number of mannose molecules that interact with the acceptor, the binding constant increases drastically to 10^6 – 10^7 L mol^{-1} .^[18] The NCs modified by NCO coupling (HES-PEG5000-C2-Man) exhibit a 200 times higher mannose density compared to HES-PEG5000-DBCO-Man and thus exposes approximately 0.55 mannose units per nm^2 . Interestingly, the binding affinity with iDCs is still low (Figure S1B). The reason for this could be that a free hydroxy group at the C-2 position of the mannose molecule is essential for interaction with the acceptor protein.^[19] Only, when 2-aminoethyl α -D-mannopyranoside (with the amine linked to the C-1 position) was used, a much stronger binding of HES-PEG5000-C1-Man to iDCs compared to unmodified and PEGylated NCs was detected (Figure S1C). These results clearly demonstrate that when mannose is attached via a PEG linker to HES-NCs with sufficient density, a multivalency effect is achieved, which enables cellular uptake into iDCs. After the successful targeting of iDCs with mannose-functionalized HES-NCs under nonphysiological conditions, the influence of human plasma on the protein interaction and targeting efficiency was studied. First, ITC was used to determine the protein interactions from human plasma with the prepared HES-NCs. The HES-NCs were titrated with diluted human plasma to measure the heat released from the protein adsorption at the surfaces after each titration step. The corresponding values were corrected for the heat of dilution. The same measurement was performed with standard polystyrene (PS) nanoparticles, which are known to exhibit a high protein binding affinity,^[20] as a reference (Figure 1).

The interactions between plasma proteins and the nanocarriers were exothermic in all cases, thus indicating protein interaction with all of the investigated NCs. However, there is a significant difference between hydrophobic PS nanoparticles and the HES-NCs: the binding affinity of the plasma

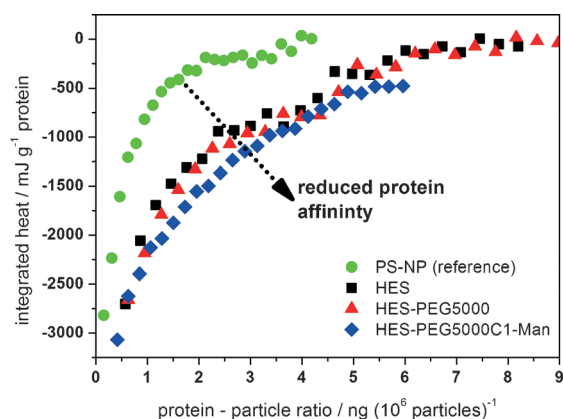


Figure 1. ITC binding isotherms for the adsorption of plasma proteins to different nanocarriers systems: unmodified HES-NCs (black ■), HES-PEG5000 NCs (red ▲), and HES-PEG5000-C1-Man NCs (blue ◆) compared to polystyrene nanoparticles (green ●) as a reference.

proteins, which is represented by the initial slope of the binding isotherm, is strongly reduced for HES-NCs. This matches the results published previously by our group and also those reported in the literature regarding the low protein affinity of HES^[21] or other carbohydrates.^[22] More interestingly, the three different HES-NCs exhibit similar protein adsorption: the ITC results show very little difference in the affinity as a result of PEGylation or additional mannose functionalization. This is an important finding since ITC gives insight into the protein corona of the NC and it indicates that the attachment of mannose does not cause significantly increased protein adsorption. Furthermore, DLS was performed in undiluted plasma to detect any aggregation of the NCs.^[23] The autocorrelation functions for the NCs/plasma mixtures can be perfectly described by the so-called force fit (Figure S2). This means that the sum of the autocorrelation functions of both individual components is kept constant with only the intensity fractions of plasma and nanocarriers as free-fit parameters.^[23] The results indicate that no structures larger than the largest size of the NCs or plasma components are formed in the mixture. However, it has to be mentioned that size distribution changes caused by a monolayer of adsorbed proteins on the NC surface cannot be detected by this method.^[24] The DLS results thus prove that no larger aggregates of NCs caused by interaction with proteins are observed. In combination with the ITC results, the most probable scenario would be a minor amount of protein adsorbed to the NC surface to partially cover the surface of the NCs. This is further supported by protein quantification and SDS-PAGE (Figure S3). Both methods indicate low overall protein adsorption on all of the HES-NCs in comparison to reference PS-NPs.

More importantly, proteomic mass spectrometry data show that the protein pattern identified is rather similar for the different NCs but different to the PS-control sample, which is a promising prerequisite for specific targeting in plasma (Figure 2). A comparable composition of the protein corona was identified on all of the HES-NCs. Only the PEGylated NCs show a slight difference with an overall lower

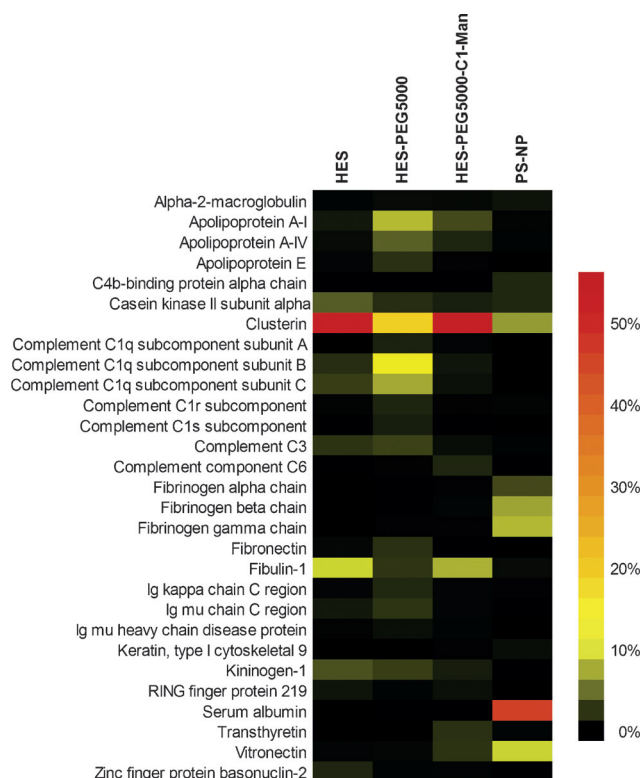


Figure 2. Heatmap of the most abundant proteins in the protein corona of HES-NC, HES-PEG5000 NCs, HES-PEG5000-C1-Man NCs and a reference PS-NP as determined by quantitative liquid chromatography coupled with mass spectrometry. Only those proteins which constitute at least 1 % of the protein corona on one of the nanocarriers are shown. Values were calculated from the molar masses of each protein.

protein adsorption (Figure 2 and Figure S3). Importantly, the protein adsorption cannot be suppressed completely in any of the cases. In order to demonstrate the accessibility of the mannose units, specific binding to C-type lectin was analyzed. The assay was performed before and after incubation with human plasma (Figure 3).

Neither unmodified HES-NCs nor PEGylated HES-NCs show any specific binding to C-type lectin before or after incubation in human plasma (the negative control without NCs has the same readout). The mannose-functionalized HES-NCs exhibit binding to the enzyme, however, the protein corona influenced the binding of C-type lectin: with adsorbed plasma proteins, the binding of C-type lectin is reduced but clear binding can still be detected (Figure 3). Combined with the data from MS, this strongly indicates that the stealth properties of the PEG layer with mannose attached at the outer layer allow control of the biological identity of the nanocarrier to specifically target DCs. Owing to their role in the immune system, the targeting of immature dendritic cells (iDCs) is biologically significant. However, as phagocytosis cells, iDCs are known to also take up NCs unspecifically. In order to verify that after adsorption of plasma proteins, the uptake of mannose-functionalized HES-NCs into DCs is a real receptor-mediated phenomenon, mature dendritic cells (mDCs) were also investigated. mDCs

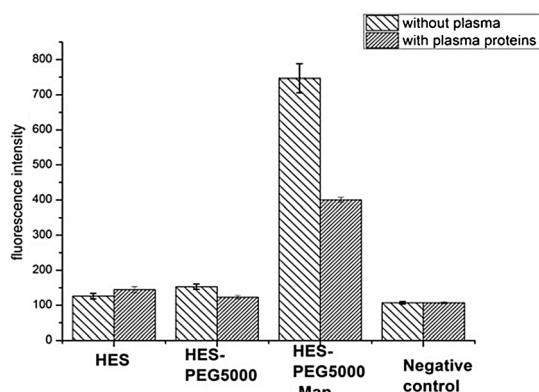


Figure 3. Binding of unmodified (HES), PEGylated (HES-PEG5000), and mannose-functionalized (HES-PEG5000-C1-Man) HES-NCs to C-type lectin before or after incubation with human plasma (the negative control was measured without the addition of HES-NCs).

have a much lower ability to function as phagocytic cells and receptor-mediated uptake was clearly demonstrated.

Figure 4 shows a similar uptake of HES-PEG5000-C1-Man into mDCs before (Figure 4A) and after (Figure 4B) incubation with human plasma (Figure S5 shows the corresponding microscopy images). These results demonstrate that PEGylated nanocarriers can be further functionalized with

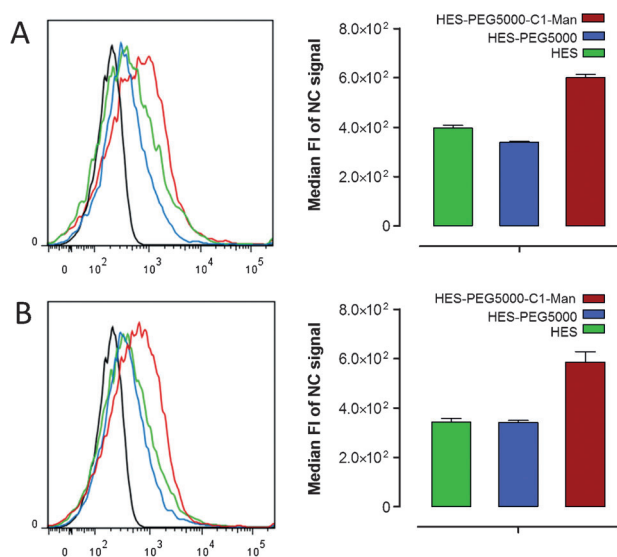


Figure 4. In vitro binding of HES-NCs to mature dendritic cells before (A) and after (B) incubation with human plasma. Mature dendritic cells were incubated with 150 $\mu\text{g mL}^{-1}$ of HES, HES-PEG5000, and HES-PEG5000-C1-Man for 2 h at 37°C. Cell uptake was analyzed by flow cytometry. Preincubation of NCs with plasma (B) has little influence on cell uptake. Histograms (left): Black line = untreated mDCs; green line = HES; blue line = HES-PEG5000; red line = HES-PEG-C1-Man.

targeting groups, for example, mannose, in order to specifically reach both immature and mature dendritic cells, even in the presence of plasma proteins. The interaction between plasma proteins and surface-bound mannose does not prevent it from being recognized by specific acceptors. This finding is in accordance with other works demonstrating minor protein

adsorption to polysaccharides including HES,^[25] chitosan,^[26] hyaluronic acid.^[27]

In conclusion, hydroxyethyl starch nanocarriers were efficiently PEGylated and functionalized at the outer-layer with amino derivatives of mannose by a convenient two-step method that relies on sequential nucleophilic additions to isocyanates. The influence of mannose attached to the PEGylated NCs on the pattern of the protein corona after plasma incubation was shown to be minimal by ITC, DLS, SDS-PAGE, and mass spectrometry. Furthermore, cellular uptake of the NCs by dendritic cells and a binding assay with C-type lectin showed that the targeting moieties are accessible to the biological receptors after incubation with plasma. Taking into consideration that rather simple carbohydrates like the disaccharide in bleomycin^[15] have been proven to be able to selectively target cancer cells, the use of a combination of stealth nanocarriers with saccharide-based targeting moieties could overcome the problem of losing the stealth effect after the coupling of other targeting agents.

Keywords: calorimetry · carbohydrates · drug delivery · nanoparticles · proteins

- a) A. Salvati, A. S. Pitek, M. P. Monopoli, K. Prapainop, F. B. Bombelli, D. R. Hristov, P. M. Kelly, C. Aberg, E. Mahon, K. A. Dawson, *Nat. Nanotechnol.* **2013**, *8*, 137–143; b) B. P. Pablo del Pino, Q. Zhang, P. Maffre, G. U. Nienhaus, W. J. Parak, *Mater. Horiz.* **2014**, *1*, 301–313.
- a) T. Cedervall, I. Lynch, S. Lindman, T. Berggard, E. Thulin, H. Nilsson, K. A. Dawson, S. Linse, *Proc. Natl. Acad. Sci. USA* **2007**, *104*, 2050–2055; b) P. Aggarwal, J. B. Hall, C. B. McLeland, M. A. Dobrovolskaia, S. E. McNeil, *Adv. Drug Delivery Rev.* **2009**, *61*, 428–437; c) D. Walczyk, F. B. Bombelli, M. P. Monopoli, I. Lynch, K. A. Dawson, *J. Am. Chem. Soc.* **2010**, *132*, 5761–5768; d) C. Röcker, M. Poetzel, F. Zhang, W. J. Parak, G. U. Nienhaus, *Nat. Nanotechnol.* **2009**, *4*, 577–580; e) Z. J. Deng, M. Liang, M. Monteiro, I. Toth, R. F. Minchin, *Nat. Nanotechnol.* **2011**, *6*, 39–44; f) C. D. Walkey, W. C. W. Chan, *Chem. Soc. Rev.* **2012**, *41*, 2780–2799; g) M. P. Monopoli, D. Walczyk, A. Campbell, G. Elia, I. Lynch, F. B. Bombelli, K. A. Dawson, *J. Am. Chem. Soc.* **2011**, *133*, 2525–2534; h) A. Albanese, C. D. Walkey, J. B. Olsen, H. Guo, A. Emili, W. C. W. Chan, *ACS Nano* **2014**, *8*, 5515–5526; i) M. S. K. Mohr, G. Baier, S. Schöttler, P. Okwieka, S. Tenzer, K. Landfester, V. Mailänder, M. Schmidt, R. G. Meyer, *J. Nanomed. Nanotechnol.* **2014**, *5*, 1000193–1000203; j) S. Tenzer, D. Docter, J. Kuharev, A. Musyanovych, V. Fetz, R. Hecht, F. Schlenk, D. Fischer, K. Kiouptsi, C. Reinhardt, K. Landfester, H. Schild, M. Maskos, S. K. Knauer, R. H. Stauber, *Nat. Nanotechnol.* **2013**, *8*, 772–U1000; k) A. Cifuentes-Rius, H. de Puig, J. C. Y. Kah, S. Borros, K. Hamad-Schifferli, *ACS Nano* **2013**, *7*, 10066–10074; l) R. Gaspar, *Nat. Nanotechnol.* **2013**, *8*, 79–80; m) C. C. Fleischer, C. K. Payne, *Acc. Chem. Res.* **2014**, *47*, 2651–2659; n) R. Tedja, M. Lim, R. Amal, C. Marquis, *ACS Nano* **2012**, *6*, 4083–4093; o) C. D. Walkey, J. B. Olsen, F. Song, R. Liu, H. Guo, D. W. H. Olsen, Y. Cohen, A. Emili, W. C. W. Chan, *ACS Nano* **2014**, *8*, 2439–2455; p) G. Y. Tonga, K. Saha, V. M. Rotello, *Adv. Mater.* **2014**, *26*, 359–370; q) M. P. Monopoli, C. Aberg, A. Salvati, K. A. Dawson, *Nat. Nanotechnol.* **2012**, *7*, 779–786; r) I. Lynch, A. Salvati, K. A. Dawson, *Nat. Nanotechnol.* **2009**, *4*, 546–547.

- [3] a) Q. Dai, C. Walkey, W. C. W. Chan, *Angew. Chem. Int. Ed.* **2014**, *53*, 5093–5096; *Angew. Chem.* **2014**, *126*, 5193–5196; b) C. D. Walkey, J. B. Olsen, H. Guo, A. Emili, W. C. W. Chan, *J. Am. Chem. Soc.* **2012**, *134*, 2139–2147.
- [4] M. Lundqvist, J. Stigler, G. Elia, I. Lynch, T. Cedervall, K. A. Dawson, *Proc. Natl. Acad. Sci. USA* **2008**, *105*, 14265–14270.
- [5] Z. J. Deng, G. Mortimer, T. Schiller, A. Musumeci, D. Martin, R. F. Minchin, *Nanotechnology* **2009**, *20*, 455101.
- [6] S. Tenzer, D. Docter, S. Rosfa, A. Wlodarski, J. Kuharev, A. Rekik, S. K. Knauer, C. Bantz, T. Nawroth, C. Bier, J. Sirirattanapan, W. Mann, L. Treuel, R. Zellner, M. Maskos, H. Schild, R. H. Stauber, *ACS Nano* **2011**, *5*, 7155–7167.
- [7] a) E. Casals, T. Pfaller, A. Duschl, G. J. Oostingh, V. Puentes, *ACS Nano* **2010**, *4*, 3623–3632; b) L. Wang, J. Li, J. Pan, X. Jiang, Y. Ji, Y. Li, Y. Qu, Y. Zhao, X. Wu, C. Chen, *J. Am. Chem. Soc.* **2013**, *135*, 17359–17368; c) A. K. Murthy, R. J. Stover, W. G. Hardin, R. Schramm, G. D. Nie, S. Gourisankar, T. M. Truskett, K. V. Sokolov, K. P. Johnston, *J. Am. Chem. Soc.* **2013**, *135*, 7799–7802.
- [8] A. S. Karakoti, S. Das, S. Thevuthasan, S. Seal, *Angew. Chem. Int. Ed.* **2011**, *50*, 1980–1994; *Angew. Chem.* **2011**, *123*, 2024–2040.
- [9] D. F. Moyano, K. Saha, G. Prakash, B. Yan, H. Kong, M. Yazdani, V. M. Rotello, *ACS Nano* **2014**, *8*, 6748–6755.
- [10] G. Baier, D. Baumann, J. M. Siebert, A. Musyanovych, V. Mailaender, K. Landfester, *Biomacromolecules* **2012**, *13*, 2704–2715.
- [11] B. Kang, P. Okwieka, S. Schottler, O. Seifert, R. E. Kontermann, K. Pfizenmaier, A. Musyanovych, R. Meyer, M. Diken, U. Sahin, V. Mailaender, F. R. Wurm, K. Landfester, *Biomaterials* **2015**, *49*, 125–134.
- [12] J. Sudimack, R. J. Lee, *Adv. Drug Delivery Rev.* **2000**, *41*, 147–162.
- [13] K. El-Boubbou, D. C. Zhu, C. Vasileiou, B. Borhan, D. Prosperi, W. Li, X. Huang, *J. Am. Chem. Soc.* **2010**, *132*, 4490–4499.
- [14] a) R. Kikkeri, B. Lepenies, A. Adibekian, P. Laurino, P. H. Seeberger, *J. Am. Chem. Soc.* **2009**, *131*, 2110–2112; b) H. Freichels, M. Wagner, P. Okwieka, R. G. Meyer, V. Mailaender, K. Landfester, A. Musyanovych, *J. Mater. Chem. B* **2013**, *1*, 4338–4348.
- [15] Z. Yu, R. M. Schmaltz, T. C. Bozeman, R. Paul, M. J. Rishel, K. S. Tsosie, S. M. Hecht, *J. Am. Chem. Soc.* **2013**, *135*, 2883–2886.
- [16] R. Herrington, K. Hock, *Flexible Polyurethane Foams*, 2nd ed., The Dow Chemical Company, **1998**.
- [17] P. Böhlen, S. Stein, W. Dairman, S. Udenfriend, *Arch. Biochem. Biophys.* **1973**, *155*, 213–220.
- [18] a) P.-H. Liang, S.-K. Wang, C.-H. Wong, *J. Am. Chem. Soc.* **2007**, *129*, 11177–11184; b) E. A. Smith, W. D. Thomas, L. L. Kiesling, R. M. Corn, *J. Am. Chem. Soc.* **2003**, *125*, 6140–6148.
- [19] N. Shibuya, I. J. Goldstein, E. J. M. Vandamme, W. J. Peumans, *J. Biol. Chem.* **1988**, *263*, 728–734.
- [20] G. Baier, C. Costa, A. Zeller, D. Baumann, C. Sayer, P. H. H. Araujo, V. Mailaender, A. Musyanovych, K. Landfester, *Macromol. Biosci.* **2011**, *11*, 628–638.
- [21] a) A. Besheer, J. Vogel, D. Glanz, J. Kressler, T. Groth, K. Maeder, *Mol. Pharm.* **2009**, *6*, 407–415; b) C. Lemarchand, R. Gref, P. Couvreur, *Eur. J. Pharm. Biopharm.* **2004**, *58*, 327–341; c) M. Orlando, Ph.D. Thesis, University of Giessen, **2003**.
- [22] a) R. E. Marchant, S. Yuan, G. Szakalasgratzl, *J. Biomater. Sci. Polym. Ed.* **1994**, *6*, 549–564; b) E. Osterberg, K. Bergstrom, K. Holmberg, T. P. Schuman, J. A. Riggs, N. L. Burns, J. M. Vanalstine, J. M. Harris, *J. Biomed. Mater. Res.* **1995**, *29*, 741–747.
- [23] K. Rausch, A. Reuter, K. Fischer, M. Schmidt, *Biomacromolecules* **2010**, *11*, 2836–2839.
- [24] M. Hemmelmann, K. Mohr, K. Fischer, R. Zentel, M. Schmidt, *Mol. Pharm.* **2013**, *10*, 3769–3775.
- [25] M. Noga, D. Edinger, R. Klaeger, S. V. Wegner, J. P. Spatz, E. Wagner, G. Winter, A. Besheer, *Biomaterials* **2013**, *34*, 2530–2538.
- [26] X. Zhang, Q. Zhang, Q. Peng, J. Zhou, L. Liao, X. Sun, L. Zhang, T. Gong, *Biomaterials* **2014**, *35*, 6130–6141.
- [27] L. Liu, H. He, M. Zhang, S. Zhang, W. Zhang, J. Liu, *Biomaterials* **2014**, *35*, 8002–8014.

Received: March 14, 2015

Published online: ■■■■■, ■■■■■

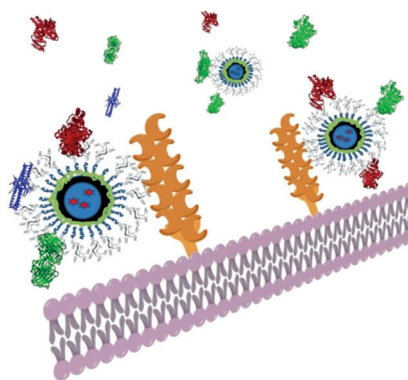
Communications



Nanocarriers

B. Kang, P. Okwieka, S. Schöttler,
S. Winzen, J. Langhanki, K. Mohr,
T. Opatz, V. Mailänder, K. Landfester,*
F. R. Wurm* ————— ■■■■—■■■■

Carbohydrate-Based Nanocarriers
Exhibiting Specific Cell Targeting with
Minimum Influence from the Protein
Corona



Stealth nanocarriers: The blood plasma interactions and targeting properties of PEGylated and mannose-functionalized hydroxyethyl starch (HES) nanocarriers were investigated. They exhibit colloidal stability in human plasma, low protein adsorption, a distinct protein pattern, and highly specific cellular uptake into dendritic cells both before and after contact with human plasma.